

# Eruptive scenarios of phonolitic volcanism at Teide–Pico Viejo volcanic complex (Tenerife, Canary Islands)

J. Martí · R. Sobradelo · A. Felpeto · O. García

Received: 18 April 2011 / Accepted: 17 October 2011  
© Springer-Verlag 2011

**Abstract** Recent studies on Teide–Pico Viejo (TPV) complex have revealed that explosive activity of phonolitic and basaltic magmas, including plinian and subplinian eruptions, and the generation of a wide range of pyroclastic density currents (PDCs) have also been significant. We perform a statistical analysis of the time series of past eruptions and the spatial extent of their erupted products, including lava flows, fallout and PDCs. We use an extreme value theory statistical method to calculate eruption recurrence. The analysis of past activity and extent of some well-identified deposits is used to calculate the eruption recurrence probabilities of various sizes and for different time periods. With this information, we compute several significant scenarios using the GIS-based VORIS 2 software (Felpeto et al., *J Volcanol Geotherm Res* 166:106–116, 2007) in order to evaluate the potential extent of the main eruption hazards that could be expected from TPV. The simulated hazard scenarios show that the southern flank of Tenerife is protected by Las Cañadas

caldera wall against lava flows and pyroclastic density currents, but not against ash fallout. The Icod Valley, and to a minor extent also the La Orotava valley, is directly exposed to most of TPV hazards, in particular to the gravity driven flows. This study represents a step forward in the evaluation of volcanic hazard at TPV with regard to previous studies, and the results obtained should be useful for intermediate and long-term land-use and emergency planning.

**Keywords** Teide–Pico Viejo · Tenerife · Phonolitic volcanism · Eruption recurrence · Eruptive scenarios · Hazard assessment

## Introduction

Tenerife is the largest (~2,050 km<sup>2</sup>) and most populated (>900,000 inhabitants) of the Canary Islands. As for the rest of this volcanic archipelago, its mild climate and impressive volcanic landscapes, including the dormant Teide and Pico Viejo complex (TPV), have contributed to make it one of the main tourist destinations in Europe with more than five million visitors per year. The presence of recurrent historical volcanism on this island is a convincing reason to undertake volcanic hazard assessment for risk-based decision-making in land-use planning and emergency management and, consequently, to improve the security of its inhabitants and its numerous visitors.

The main concern about potential future volcanic activity on Tenerife has traditionally been addressed towards basaltic eruptions taking place along the two active rift zones, as they have occurred in historical times (Carracedo et al. 2007, 2010). However, despite the occurrence of numerous eruptions during the Holocene

Editorial responsibility: S. Nakada

J. Martí (✉) · R. Sobradelo  
Institute of Earth Sciences “Jaume Almera”, CSIC,  
Lluís Solé Sabarís s/n,  
08028 Barcelona, Spain  
e-mail: joan.marti@ija.csic.es

A. Felpeto  
Observatorio Geofísico Central,  
Instituto Geográfico Nacional (IGN),  
c/Alfonso XII, 3,  
28014 Madrid, Spain

O. García  
Centro Geofísico de Canarias,  
Instituto Geográfico Nacional (IGN),  
c/La Marina 20, 2°,  
38001 Santa Cruz de Tenerife, Spain

(Carracedo et al. 2007) and of unequivocal signs of activity in historical times (fumaroles, seismicity) (IGN seismic catalogue) and even an unrest episode in 2004 (García et al. 2006; Pérez et al. 2005; Gottsmann et al. 2006; Martí et al. 2009; Domínguez Cerdeña et al. 2011), TPV has not been considered as a major threat.

Although the highest probability of having a new eruption on Tenerife corresponds to a basaltic eruption along the rift zones, which today would also represent a significant trouble for the island, the probability of having a new eruption from the TPV central complex is not negligible. This is indicated by the number of eruptions that it has produced during the Holocene (see Carracedo et al. 2007), most of them of phonolitic composition and triggered by intrusion of deep basaltic magma into shallow felsic magma chambers (Martí et al. 2008a).

The complexity of any volcanic system and its associated eruptive processes, together with the lack of data that characterises many active volcanoes, particularly those with long periods between eruptions, makes volcanic hazard quantification very challenging, as there is often not enough observational data to build a robust statistical model. This is the case for TPV, about which information on their past eruptive history and its present state of activity is still incomplete. This restricts the existing techniques for forecasting its future behaviour to within a minimum margin of confidence. However, different efforts have been made to assess volcanic hazard at TPV in the form of event tree structures representing possible eruptive scenarios and using the available geological and geophysical information (Martí et al. 2008b; Sobradelo and Martí 2010). Bayesian inference and expert judgement elicitation techniques have been applied to these event trees to estimate the long-term probability for each scenario within a given time window. This has allowed us to rationalise our current knowledge of TPV and provides a tool for understanding and anticipating the future behaviour of these volcanoes. These previous studies have not yet, however, been able to quantify the recurrence and extent for each possible scenario.

In order to move one step forward in the hazard assessment at TPV, it is important to estimate the temporal and spatial probability of an eruption for various time windows in the near future and study in detail-specific eruptive scenarios for each of the main associated hazards. This study focusses on phonolitic volcanism, as it has been clearly dominant at TPV through the Holocene and also because it would produce the most hazardous scenarios. In this paper, we first do a threat analysis of the TPV complex using the Ewert et al. (2005) template in order to compare them with other volcanoes of similar characteristics. Then we calculate the temporal and spatial probability of a phonolitic eruption from TPV using available data. After that, we computed several significant scenarios using the

GIS-based VORIS 2 software (Felpeto et al. 2007) in order to evaluate the potential extent of the main eruption hazards expected from TPV. Finally, we discuss the results obtained and compare them with the Bayesian technique previously applied to estimate the long-term hazard. The elaboration of a quantitative hazard map for the whole island of Tenerife, including a probabilistic estimate for each point of the map of being impacted by the different hazards considered, is beyond the purpose of this study and will constitute the specific goal of a new paper.

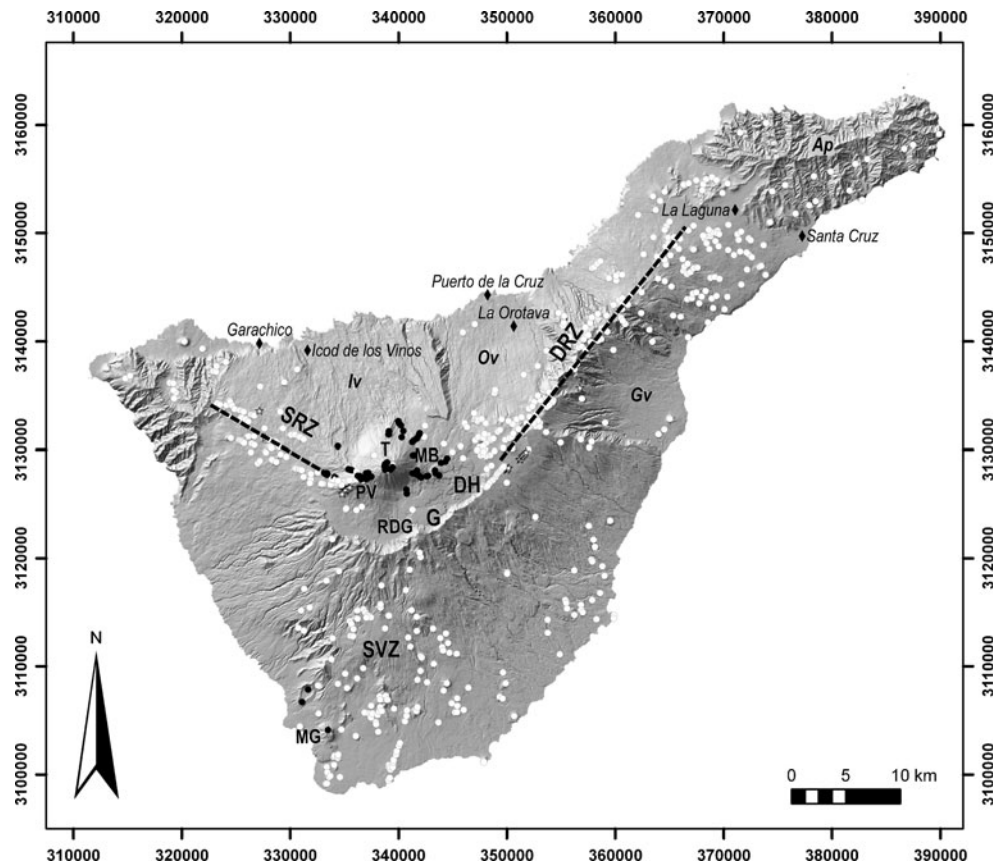
## Geological background

TPV complex is composed by the twin Teide and Pico Viejo stratovolcanoes that started to grow simultaneously at about 180–190 ka within the Las Cañadas caldera (Fig. 1), which is a volcanic depression formed by several vertical collapses of the former Tenerife central volcanic edifice (Las Cañadas edifice) following explosive emptying of a high-level magma chamber. Occasional lateral collapses of the volcano flanks also occurred and modified the resulting caldera depression (Martí et al. 1994, 1997; Martí and Gudmundsson 2000). The construction of the present central volcanic complex on Tenerife encompasses the formation of these twin strato-volcanoes, which derive from the interaction of two different shallow magma systems that evolved simultaneously, giving rise to a complete series from basalt to phonolite (Ablay et al. 1998; Martí et al. 2008a).

The structure and volcanic stratigraphy of the TPV was characterised by Ablay and Martí (2000), based on a detailed field and petrological study. Later, Carracedo et al. (2003, 2007) provided the first group of isotopic ages from TPV products, and Martí et al. (2008a) analysed the potential for future TPV activity. More recently, García et al. (2011) identified the products of several explosive eruptions of phonolitic composition from these volcanoes. The reader will find in these works more complete descriptions of the stratigraphic and volcanological evolution of TPV.

TPV mostly consists of mafic to intermediate products, with felsic materials volumetrically subordinate overall (see Martí et al. 2008a). Felsic products, however, dominate the recent output of the TPV system. Eruptions at TPV have occurred from their central vents but also from a multitude of vents distributed on their flanks (Fig. 1). Mafic and phonolitic magmas have been erupted from these vents. The Santiago del Teide and Dorsal rift axes (Fig. 1), the two main tectonic lineations currently active on Tenerife, probably join beneath TPV complex (Carracedo 1994; Ablay and Martí 2000). Some flank vents at the western side of Pico Viejo are located on eruption fissures that are sub-parallel to fissures further down the Santiago del Teide

**Fig. 1** Simplified geological and topographic map of Tenerife illustrating the general distribution of visible vents. *Black symbols* mafic and intermediate vents; *white symbols* felsic vents; *stars* historic and sub-historic vents; *circles* other vents. *Grey squares* some main population centres. *DH* Diego Hernández, *DRZ* Dorsal rift zone, *G* Guajara, *MB* Montaña Blanca, *MG* Montaña Guaza, *RDG* Roques de García, *T* Teide volcano, *PV* Pico Viejo volcano, *SRZ* Santiago rift zone, *SVZ* Southern volcanic zone, *Iv* Icod valley, *Ov* Orotava valley, *Gv* Güimar valley, *Ap* Anaga peninsula (projection: UTM 28N)



rift and define the main rift axis. On the eastern side of Teide, some flank vents define eruption fissures orientated parallel to the Dorsal rift.

The eruptive history of the TPV comprises a main stage of eruption of mafic to intermediate lavas that form the core of the volcanoes and also infill most of the Las Cañadas depression and the adjacent La Orotava and Icod valleys. At about 35 ka, the first phonolites appeared, and since then, they have become the predominant composition in the TPV eruptions. Basaltic eruptions have also continued mostly associated with the two main rift zones. The available petrological data suggest that the interaction of a deep basaltic magmatic system with a shallow phonolitic magmatic one beneath central Tenerife controls the eruption dynamics of TPV (Martí et al. 2008a). Most of the phonolitic eruptions from TPV show signs of magma mixing, suggesting that eruptions were triggered by intrusion of deep basaltic magmas into shallow phonolitic reservoirs.

Phonolitic activity from TPV shows repose intervals around 250–1,000 years, according to the isotopic ages published by Carracedo et al. (2003, 2007). Phonolitic eruptions from TPV range in volume from 0.01 to  $>1 \text{ km}^3$  and mostly produce thick clastogenic lava flows and domes, occasionally associated with explosive episodes ranging from subplinian to plinian, which have generated

extensive pumice fall deposits and PDCs (Ablay et al. 1995; Martí et al. 2008a; García et al. 2011). The emplacement of clastogenic lava flows and domes have also generated explosive episodes when block and ash flows were generated by gravitational collapses (García et al. 2011).

Some significant basaltic eruptions have occurred as well from the flanks or the central vents of TPV. All basaltic eruptions have developed explosive strombolian to violent strombolian phases leading to the construction of scoria cones and occasionally producing intense lava fountaining and violent explosions with the formation of ash-rich eruption columns. Violent basaltic phreatomagmatic eruptions have also occurred from the central craters of the TPV, generating high-energy, pyroclastic density currents. Table 1 summarises 16 phonolitic eruptions documented geologically for TPV during Holocene.

### Threat analysis

Quantification of the threat posed by volcanoes is an important issue when trying to define the monitoring level required by each volcano, especially in comparison with others. Ewert et al. (2005) developed the National Volcano

**Table 1** TPV Holocene phonolitic eruptions

Event ID	Eruption Name	Years BP	Total erupted DRE (m <sup>3</sup> )	Total erupted mass (kg)	Magnitude scale
1	Montaña Reventada	895	138,194,471.1	3.45486E+11	4.5384
2	Lavas Negras	1,150	474,452,978	1.18613E+12	5.0741
3	Roques Blancos	1,714–1,790	833,890,093.4	2.08473E+12	5.3190
4	Montaña Blanca	2,020	107,382,578.7	2.68456E+11	4.4289
5	Montaña Majua	3,520?	69,744,811.59	1.74362E+11	4.2415
6	El Boqueron	2,528–5,660	44,283,790.64	1.10709E+11	4.0442
7	Cañada Blanca	2,528–5,911	70,115,211.27	1.75288E+11	4.2438
8	Abejera Baja	5,486	285,594,326	7.13986E+11	4.8537
9	Abejera Alta	5,911	361,123,567.2	9.02809E+11	4.96
10	Pico Cabras	5,911–7,900	285,594,326	7.13986E+11	4.8537
11	Abrunco	<10,000	2,086,022.525	5,215,056,313	2.7173
12	Montaña de la Cruz	<10,000	131,444,541.8	3.28611E+11	4.5167
13	Arenas Blancas	<10,000	101,381,078.6	2.53453E+11	4.4039
14	Montaña de los Conejos	≥10,000	70,723,423.92	1.76809E+11	4.2475
15	Bocas de Maria	≥10,000	23,265,710.9	58,164,277,258	3.7647
16	Montaña Las Lajas	≥10,000	10,769,291.55	26,923,228,872	3.4301

Ages from Carracedo et al. (2007) and Olaya García (unpublished data)

Early Warning System (NVEWS) intending to assess the threat posed by US volcanoes, proposing an analysis scheme based on several factors. These factors can be divided into two main groups: those associated with hazard and those associated with exposure of human, social and economical elements potentially affected by the hazard, i.e. with risk. The product of the sums of all the factors of each type gives a threat score that allows the classification of the US volcano in four categories, grouped by the required monitoring level.

Other authors have applied NVEWS analysis to other volcanoes, such as Kinvig et al. (2010), who recently applied this analysis to Nysiros volcano (Greece). In this paper, we applied the NVEWS scheme in order to quantify the threat posed by TPV and to facilitate the comparison with other volcanoes. Scores given to each factor (labelled from (a) to (y)) and the total result are shown in Table 2. Brief explanations of the factors we took into account are given in the next sections, while Table 2 caption indicates how the corresponding scores were assigned and lists the bibliographic/web sources used.

#### Hazard factors

TPV includes two stratovolcanoes (a), with major explosive activity during the last 10,000 years (see Table 1) with calculated magnitudes up to 5. In a few cases where associated pyroclastic fall deposits have been preserved, it has been also possible to estimate a Volcanic Explosivity Index (VEI) value, which combines magnitude, intensity (eruption rate) and explosivity (eruption column high) of

the eruption (Newhall and Self 1982), for these particular cases, which ranges from 3 to 4 (b) (d) (see below). The historical period of Tenerife is relatively short as it starts with the conquering of the island by the Spanish crown in 1496. Since then, four eruptions (all of them basaltic) have occurred on the island, only one on TPV (1798, Chahorra eruption). During the Holocene, at least 16 phonolitic eruptions occurred in TPV as shown in Table 1 (e), including most of the volcanic hazards: pyroclastic flows, lava flows, lahars... (f)(g)(h), although there is no evidence for a volcanic tsunami (j). TPV hydrothermal systems are large enough to justify its potential for hydrothermal explosions (i). This fact plus the steep slopes of their flanks and their history of sector collapses (Ably and Martí 2000) show its potential for new sector collapses (k). In 2004–2005, an episode of volcanic unrest took place in the island of Tenerife, characterised by a great increase on the seismic activity around the TPV system and changes in the fumarolic system (m)(o).

#### Exposure factors

The first exposure factor measures the population in a circle of 30 km centred on the volcano. This circle centred on TPV comprises most of Tenerife Island, leaving out only the Anaga peninsula, which includes the two most populated municipalities of the island (Santa Cruz and San Cristóbal de la Laguna), so almost the same population lives inside and outside the circle. Based on public data published by the National Institute of Statistics (<http://www.ine.es>) for 2009, the population included in the circle is

**Table 2** TPV NVEWS scoring factors

		Scoring ranges
Teide–Pico Viejo hazard factors		
(a)	Volcano type	1
(b)	Maximum Volcanic Explosivity Index	1
(c)	Explosive activity in past 500 years?	0
(d)	Major explosive activity in past 5,000 years?	1
(e)	Eruption recurrence	1
(f)	Holocene pyroclastic flows?	1
(g)	Holocene lahars?	1
(h)	Holocene lava flow?	1
(i)	Hydrothermal explosion potential?	1
(j)	Holocene tsunami?	0
(k)	Sector collapse potential?	1
(l)	Primary lahar source?	0
(m)	Observed seismic unrest?	1
(n)	Observed ground deformation?	0
(o)	Observed fumarolic or magmatic degassing?	1
	Total of hazard factors	11
Teide–Pico Viejo exposure factors		
(p)	Log <sub>10</sub> of Volcano Population Index at 30 km	4
(q)	Log <sub>10</sub> of approximate population downstream or downslope	0
(r)	Historical fatalities?	0
(s)	Historical evacuations?	0
(t)	Local aviation exposure	2
(u)	Regional aviation exposure	5
(v)	Power infrastructure	1
(w)	Transportation infrastructure	1
(x)	Major development or sensitive areas	1
(y)	Volcano is a significant part of a populated island	1
	Total of exposure factors	15
	Sum of all hazard factors×Sum of all exposure factors=Relative threat ranking	165

We tried to use conservative values for the scores of each factor in order to minimise the uncertainty caused by the lack of data in some cases, so that the threat score obtained is a minimum. (a) Volcano type tries to quantify how dangerous a volcano is and has two categories: type 0 volcanoes, including cinder cones, basaltic volcanic fields, shields, tuff rings and fissure vents, and type 1 volcanoes which are generally more explosive, including stratovolcanoes, lava domes, complex volcanoes, maars and calderas. (b) The VEI is an indicator of the explosive character and size of an eruption (Newhall and Self 1982). In the NVEWS scheme, the scores are 1 for VEI of 3–4, 2 for a VEI of 5–6 and 3 for a VEI of 7–8. (c) Explosive activity and (d) major explosive activity refer to the presence of repeated explosive episodes in the past eruptions record, as scores as 1 for VEI $\geq$ 3 within the last 500 years and VEI $\geq$ 4 within the last 5,000 years, respectively. (e) Eruption recurrence: It scores 4 if the eruption interval is 1–99 years, 3 if it is 100–1,000, 2 if it 1,000 to several thousands, 1 if eruption interval is 5,000–10,000 years and 0 if there are not Holocene eruptions. For factors (f) to (o), possible scores are 1 or 0 if the answer is yes or not, respectively (see Ewert et al. 2005 for more details). For exposure factors and their possible scores, see text and Ewert et al. (2005, p. 47). Information sources: (a) Ablay and Martí (2000); (b) García et al. (2011); (c)–(e) Carracedo et al. (2007); (f)–(h) Martí et al. (2008b) and García et al. (2011); (i) Del Potro and Hurlimann (2008) and Rodríguez Losada et al. (2009); (k) Ablay and Martí (2000) and Ablay and Hurlimann (2000); (m) Spanish Geographical Institute (<http://www.ign.es>), García et al. (2006) and Martí et al. (2009); (o) Hernández et al. (1998), Pérez et al. (2005) and Martí et al. (2009); (p) Spanish National Institute of Statistics (<http://www.ine.es>); (t)–(u) Association of Spanish Airports (<http://www.aena.es>)

about 442,000. However, Tenerife is one of the main tourist destinations of Europe, so the touristic population should also be taken into account. During 2009, the mean daily hotel occupancy in the island was about 52,000 tourists, so the value of (p) factor can reach 5 (see Table 2). There is

almost no difference in the population downstream of the volcano that lies beyond, versus within, the above-mentioned circle.

No fatalities have been recorded during eruptions at Tenerife. A massive evacuation occurred during 1706,

when basaltic lava flows almost destroyed Garachico, the former capital of the island, but that basaltic eruption had its vent on the Santiago rift, not on TPV (s).

TPV poses a significant threat to aviation, as all the eight Canarian airports fall in a circle of 300 km radius centred between the two stratovolcanoes. The mean number of daily passengers in this circle was around 82,200 during 2009 (t)(u). The Canary Islands constitute one of the main civil aviation corridors for flights from Europe to Central and South America and vice versa.

### Evaluation of temporal and spatial probability of a phonolitic eruption in TPV

#### Temporal probability

Mid-/long-term assessment of the temporal probability of occurrence of a volcanic eruption of certain (or exceeding a) magnitude or size is usually computed by analysing the sequence of past eruptions in a volcano and characterising them by a measure of their size or magnitude (Pyle 2000). This may be indicated as magnitude, understanding it as a measure of the total volume of magma erupted, or as VEI. Unfortunately, only a small proportion of eruptions have been witnessed, so for most cases the data required to estimate the size of an eruption have to be collected in the field from physical volcanology studies of the eruption products. An additional complexity comes from the fact that it is very common that the record of volcanic eruptions is incomplete, especially for the pre-historical section of the record and the low-magnitude eruptions, and this may significantly affect the accuracy and completeness of the reconstruction of the volcano's eruption record.

In the case of TPV, at least 16 phonolitic eruptions can be identified on stratigraphic and geochronological bases in the Holocene (Carracedo et al. 2007; Martí et al. 2008a; Olaya Garcia, unpublished data, 2011). At least 15 of these eruptions were of magnitude  $M$  greater than 3, based on minimum volumes exposed (Table 1) and applying the equation proposed by Pyle (2000) to calculate the magnitude scale as follows:

$$\text{Magnitude}(M) = \log_{10}(\text{total erupted mass, kg}) - 7 \quad (1)$$

For example, the magnitude for the first eruption in Table 1 "Montaña Reventada" is  $M = \log_{10}(3.45486E+ 11) - 7 = 4.5384$ . Some of these eruptions also included explosive phases that generated fall deposits of different extents and thicknesses. Despite the poor preservation of these deposits, their characterisation in terms of grain size and thickness variations has allowed us to assign a minimum VEI value to each of them. It was not possible to determine with

precision the total volume corresponding to the fall deposits, so the total volume of erupted magma (magnitude) for the eruptions including effusive and explosive phases was probably underestimated compared to those volumes for eruptions without associated fall deposits. The absence of pyroclastic deposits does not necessarily mean that these other eruptions were not explosive at all, as it is also possible that the corresponding pyroclastic deposits could have been completely eroded. For this reason, we used  $M$ , principally based on the volume of lavas exposed, instead of VEI, as it offers a better estimate of the minimum size of the TPV eruptions and allows comparisons among them.

In this paper, we used a non-homogeneous Poisson process with a generalized Pareto distribution (GPD) as an intensity function (NHGPPP) to model the TPV time series and compute the temporal probabilities of at least one eruption in a given time interval (Coles 2001; Mendoza-Rosas and De la Cruz-Reyna 2008; Sobradelo et al. 2011). NHGPPP is an extreme value theory statistical method, very robust for modelling small time series of incomplete geological records and useful for obtaining estimates of the probability of intermediate- to high-magnitude eruption events (Coles 2001). We used this method because the incomplete geological record of the eruption products from TPV requires an estimation technique that is not very sensitive to the fact that we have a small dataset. This method is also appropriate when we have a time series of extreme values like this which is a dataset containing very few, probably incomplete, data. The GPD is a robust tool which allows modelling extreme values, such as the "rare" high-magnitude eruptions.

The fact that there is one eruption documented with  $M < 3$  and that the number of eruptions with  $M=3$  is significantly lower than those of  $M=4$  makes us believe that the catalogue may be incomplete. To account for the possible missing data or inaccuracies in the catalogue, the occurrence rates for  $M$ s 4 and 5 were used to extrapolate unobserved records using the best fit to the class VEI values of eruptions. In order to estimate these values, we used the power law described by Newhall and Self (1982), which was originally defined for VEIs but that in our case is applied to magnitudes, as higher magnitudes also imply potentially higher VEI. We therefore redefine this power law by saying that the eruption occurrence rate  $\lambda_M$  (number of eruptions per unit time) of each class  $M$  is related to the eruption size as:

$$\log \lambda_M = a - b \times M \quad (2)$$

where  $a$  and  $b$  are constants that describe the power law decay of occurrences with increasing size  $M$  over a given time interval.

In order to apply the NHGPPP, we used the exceedance over a threshold (EOT) to sample the original data; this is  $X_i > u$  for some value of  $i$ . The reader will find a complete explanation of this methodology in Coles (2001) and Mendoza-Rosas and De la Cruz-Reyna (2008). Sobradelo et al. (2011) have applied the same method to the Canary Islands historical records.

The EOT method includes all the values of the variable that exceed an a priori established threshold,  $u$ , fixed according to the model needs, providing a physically based definition of what must be considered an extreme event. The choice of the threshold value has a strong subjective component. This random variable is defined by the transformed random variable  $Y = u$ , for all  $X_i > u$  where  $Y$  is the excess over the threshold  $u$ , the  $M$  value in our case. The parameter that was used as random variable to estimate the probability of occurrence of a future eruption and thus the volcanic hazard was the time interval  $T$  between eruptions, also called repose period, together with the  $M$  size.

Figure 2 shows a scatterplot of the repose periods, where the duration of the interval  $T_{i+1}$  between two successive eruptions is plotted against the duration of the previous repose interval  $T_i$ . The diagram in Fig. 2 shows a large dispersion of points. The correlation coefficient between consecutive repose times is 0.5457, indicating a low serial correlation. We do not have enough evidence to say that consecutive repose intervals are time-dependent based on these data, so we assume independence of repose times for the purpose of this study.

For the particular case of volcanic eruptions, the size of the eruptions and the time of their occurrence are viewed as points in a two-dimensional space, which formally is the realisation of a point process. The intensity measure  $\lambda_B > u$  of this two-dimensional

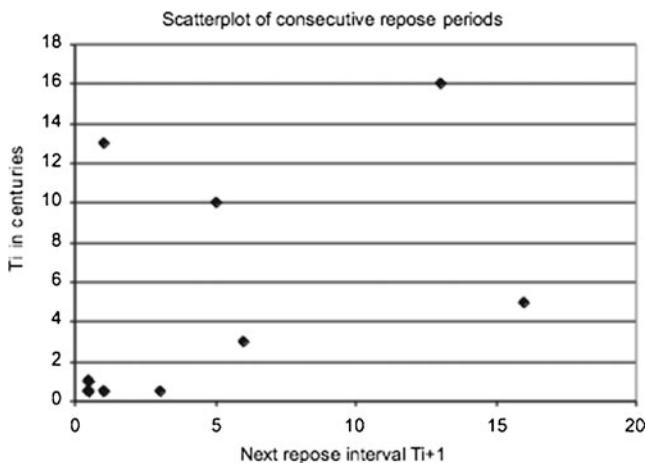


Fig. 2 Scatterplot of consecutive repose intervals for TPV time series

Poisson process on the space  $B = [t_1, t_2] \times (u, \infty)$  with  $[t_1, t_2] \subset [0, 1]$  is given by

$$\Lambda_B = (t_2 - t_1) \left( 1 - \frac{\beta(1 - u)}{\theta} \right)^{1/\beta} \tag{3}$$

where  $\beta$  and  $\theta$  are the parameters of the GPD, computed using a diagnostic method introduced by Davison and Smith (1990) which also serves to decide how well the model fits the data. This method is based on the property that the mean excess over a threshold  $u$ , for any  $u > 0$ , is a linear function of  $u$ . The mean excess is defined as

$$E(X - u | X > u) = \frac{\theta - \beta u}{1 + \beta} \tag{4}$$

for  $\beta > 1$ ,  $u > 0$  and  $(\theta - \beta u) > 0$ . The expected value was estimated using the sample mean excess computed from the data. In Fig. 3, we plot the sample mean of the excesses versus their thresholds. The x-axis is the threshold and the y-axis is the sample mean of all excesses over that threshold. As we can see, the mean excess follows a nearly straight line, with an  $R^2$  of 0.9996, suggesting a good fit. A regression line for the mean of exceedances over the threshold has been added to confirm the series follows the GPD.

Hence, according to Davison and Smith (1990), the preceding results indicate that the NHGPPP was satisfactory and appropriate to model our data. The Pareto generalized parameters for the process, derived from the regression parameters in Fig. 3 and Eq. 4, are 0.768 for shape and 5.689 for the scale. Using Eq. 2, we estimated the intensity  $\hat{\lambda}$  of the NHGPPP and obtained the probability estimations of at least one eruption of a certain  $M$  size in a given time interval. Table 3 shows the probability of having at least one eruption  $\Pr(X \geq 1)$  computed as 1 minus the probability of having no eruption  $1 - \Pr(X = 0)$  of a certain  $M$  size in a given time window, estimated using the NHGPPP with intensity rate  $\hat{\lambda}$ . To measure the volatility of the estimated

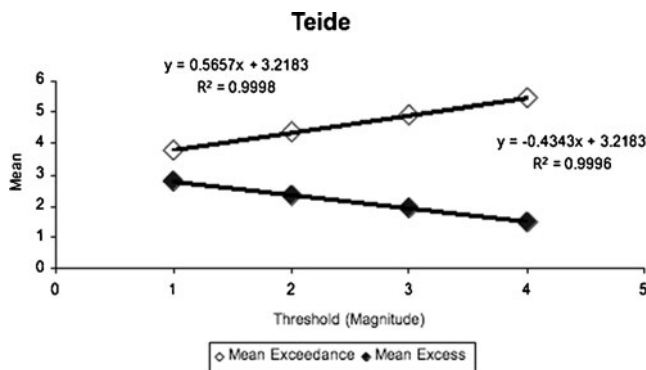


Fig. 3 Plot of exceedance and excess mean vs. threshold for TPV

**Table 3** Probability of at least one event of size  $M > x$  in the next  $t$  years in the TPV complex estimated with a NHGPPP

Years	Pr( $X=0$ ) (%)	$\hat{\lambda}$	Pr( $X \geq 1$ ) (%)	$\hat{\sigma}$
<i>M &gt; 2</i>				
1	99.8	0.002	0.2	0.0002
20	95.4	0.047	4.6	0.003
50	88.9	0.118	11.1	0.007
100	79.0	0.236	21.0	0.011
500	30.7	1.180	69.3	0.009
	1,000 0.002	09.4	2.360	90.6
<i>M &gt; 3</i>				
1	99.8	0.002	0.2	0.0001
20	96.3	0.038	3.7	0.003
50	90.9	0.095	9.1	0.006
100	82.7	0.190	17.3	0.010
500	38.6	0.951	61.4	0.011
	1,000 0.003	14.9	1.901	85.1
<i>M &gt; 4</i>				
1	99.9	0.001	0.1	0.0001
20	97.1	0.029	2.9	0.002
50	92.9	0.073	7.1	0.005
100	86.4	0.146	13.6	0.008
500	48.1	0.732	51.9	0.013
	1,000 0.006	23.1	1.464	76.9
<i>M &gt; 5</i>				
1	99.9	0.001	0.1	0.0001
20	97.9	0.021	2.1	0.002
50	94.9	0.052	5.1	0.004
100	90.0	0.105	10.0	0.007
500	59.2	0.525	40.8	0.014
	1,000 0.010	35.0	1.050	65.0
<i>M &gt; 6</i>				
1	99.9	0.001	0.1	0.0001
20	98.7	0.013	1.3	0.001
50	96.7	0.033	3.3	0.002
100	93.6	0.066	6.4	0.004
500	71.8	0.332	28.2	0.013
1,000	51.5	0.663	48.5	0.014

(Pr( $X=0$ ) and Pr( $X \geq 1$ ) are the probability of having no eruption and the probability of having at least one eruption, respectively, of a certain size in a particular time interval;  $\hat{\lambda}$  is the estimated parameter rate for the NHGPPP, and  $\hat{\sigma}$  is the estimated standard deviation for the Pr( $X \geq 1$ ) computed with the NHGPPP, based on the delta method)

probabilities, we computed the standard deviation  $\hat{\sigma}$  of the estimator using the delta method to determine its asymptotic distribution.

## Spatial probability

Felpeto et al. (2007) and Martí and Felpeto (2010) have proposed the term volcanic susceptibility for the spatial probability of vent opening. Martí and Felpeto (2010) compute this probability for long-term analysis based on a multicriteria analysis. Similarly, Marzocchi et al. (2010) in their system BET-VH compute the spatial probability based on a Bayesian approach.

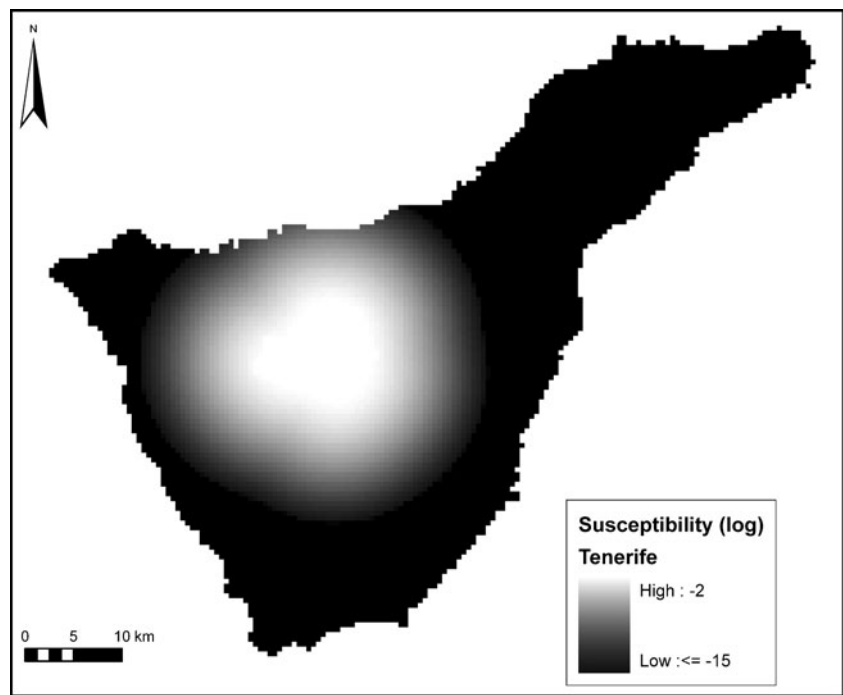
The evaluation of susceptibility of phonolitic eruptions in the island of Tenerife made by Martí and Felpeto (2010) assumed that the main stress field in the island has remained constant for the last 35 ky. The input data used were the location of felsic centres and felsic alignments younger than 35 ka, all of them belonging to TPV complex. Intensity functions for each dataset were computed separately applying the kernel technique (Connor and Hill 1995; Martin et al. 2004), and finally, the susceptibility map (Fig. 4) was computed assuming a non-homogeneous Poisson process whose intensity function is a combination of the previously calculated functions (see Martí and Felpeto 2010 for details).

## Spatiotemporal probability

Once both the temporal and the spatial probability of occurrence of a phonolitic eruption in TPV were calculated, the next step consisted in the computation of a map that, for a specific time interval  $t$  and a specific magnitude  $M$ , showed the probability for each cell of hosting a future vent. We assumed to have  $N$  possible cells that could host a future vent and that we had computed the spatial probability of each cell using the spatial probability method explained above. Let  $s_i$  be the spatial probability of a vent opening in cell  $i$ , for  $i$  ranging from 1 to  $N$ . Let  $P_{t,M}$  be the temporal probability of having an eruption (and consequently a vent opening) of magnitude  $M$  within the next  $t$  years, computed using the NHGPPP explained earlier. The group of  $N$  cells used to compute the spatial probability are mutually exclusive and exhaustive; that is, the same vent cannot be in more than one cell at the same time, and the sum of all  $s_i$  is 1.

As this paper is a first step to assess the spatiotemporal probability for TPV, for simplicity in the methodology, we assumed the two probabilities were independent. This means that the probability of having an eruption of size  $M$  in  $t$  years does not depend on the location. In other words, both the temporal and spatial probabilities were calculated separately using methods previously developed independently of one another. In this respect, we may be underestimating the total probabilities. Further work is needed to develop a more complete model which takes into account the three variables together: time, size and location.

**Fig. 4** Susceptibility map of phonolitic eruptions in Tenerife with cell size of 500×500 m (from Martí and Felpeto 2010)



The spatiotemporal probability of having an eruption of magnitude  $M$  within the next  $t$  years in cell  $i$  is:

$$qi_{t,M} = s_i \times p_{t,M} \tag{5}$$

For  $i=1, \dots, N$ ;  $M=2, 3, 4, 5, 6$ ;  $t=1, 20, 50, 100, 500, 1,000$  where

$$\sum_{i=1}^N s_i = 1 \tag{6}$$

the cells are exhaustive and

$$\sum_{i=1}^N s_i \times p_{t,M} = p_{t,M} \tag{7}$$

With the aim of obtaining the group of  $N$  cells that are mutually exclusive and exhaustive that represent TPV system, we selected from Fig. 4 the area of susceptibility values higher than  $3 \times 10^{-5}$  that encloses the 98.7% of the total probability of the susceptibility map. The values of this area were normalized by dividing by the integral across the whole area, obtaining an exhaustive group of cells. Figure 5 shows an example of how the spatiotemporal probability is computed using Eq. 5, for the probability of having an eruption of magnitude  $>2$  in the next 20 years.

**Eruptive scenarios**

In order to illustrate potential future phonolitic eruptions on TPV, we have computed several representative scenarios.

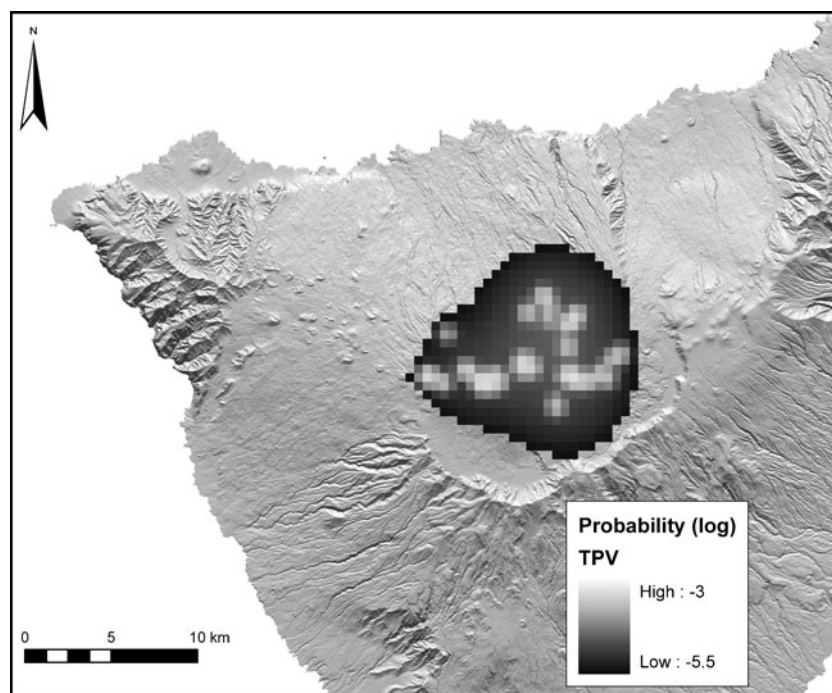
We chose lava flows, ash fall and pyroclastic density currents (PDC) as the three main hazards that can be expected in a phonolitic eruption from TPV, based on what can be seen in the geological record (Martí et al. 2008b; García et al. 2011)

Simulations were performed considering different vents, including central vents located at both craters of Teide and Pico Viejo and flank vents located around TPV edifice at approximately 2,300 m.a.s.l. Both kinds of eruptions can be expected in TPV, as shown in the Holocene eruptive record and in numerical studies simulating magma emplacement inside TPV (Martí and Geyer 2009). All the scenarios have been computed with the GIS-based system VORIS (Felpeto et al. 2007, [www.gvb-csic.es](http://www.gvb-csic.es)).

**Lava flows**

The numerical simulation of phonolitic lava flows were computed with a maximum slope model (Felpeto et al. 2001). Parameters required by the model are maximum flow length and height correction, whose values were chosen based on recent phonolitic lava flows ( $l_{max}=30$  km,  $h_c=10$  m). Simulations were performed over a digital elevation model (DEM) with 50 m of cell size. Due to the morphology of both central peaks and the characteristics of the model selected, Teide central vent was considered to be an area of  $0.17$  km<sup>2</sup> centred in the peak, and Pico Viejo central vent was considered to be an area of  $0.17$  km<sup>2</sup> around the crater rim. The result of each simulation is a probability map showing the probability of

**Fig. 5** Probability map of a phonolitic eruption  $M \geq 3$  in the next 20 years (cell size  $500 \times 500$  m). The area outside the central *black-grey* zone is assumed to have a zero probability for hosting phonolitic eruptions with  $M \geq 3$  in the next 20 years



each cell to be invaded by phonolitic lava flows. Examples of the simulations for the central vents are shown in Fig. 6.

#### *PDCs*

Numerical simulations of PDCs were computed with the energy cone model (Malin and Sheridan 1982; Sheridan and Malin 1983), over a DEM with a 50-m cell size. The values chosen for the input parameters are 200 m for equivalent collapse height and 0.21 for Heim coefficient. The result of each simulation is the area potentially

reachable by the PDC and the expected flow velocity value in each cell, computed following Toyos et al. (2007). Figure 7 shows the simulations for both central eruptions, where the potentially reachable area is very wide, and a simulation for a flank vent at the north, whose reachable area is considerably smaller.

#### *Ash fall*

Ash fall from phonolitic eruptions in TPV could be expected from different eruptive styles. Those considered

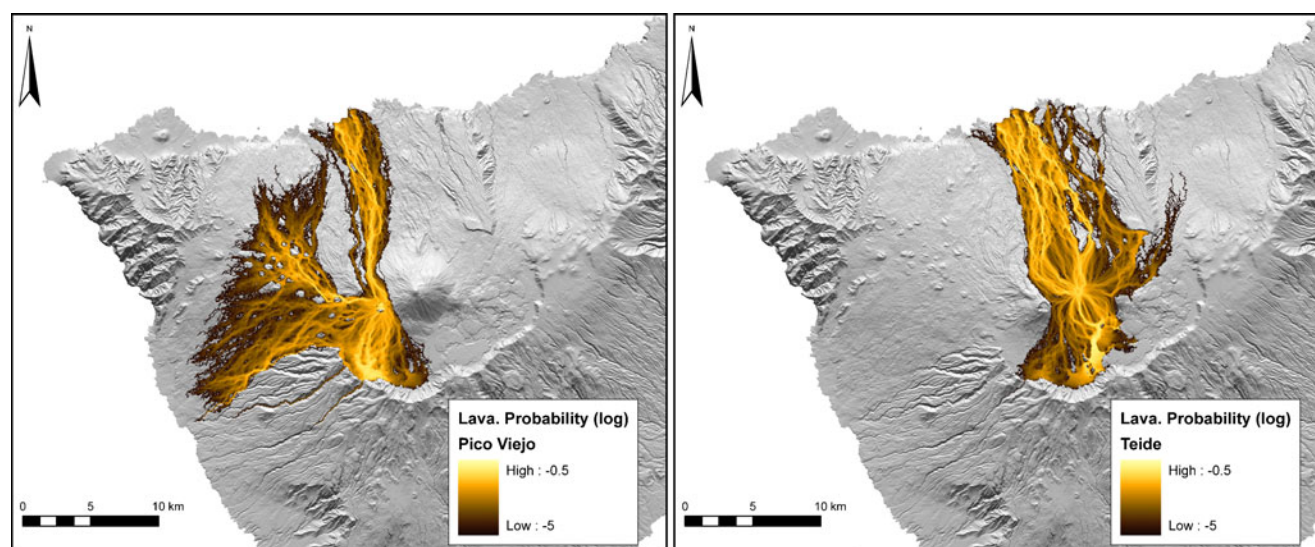


**Fig. 6** Phonolitic lava flow scenarios for Pico Viejo (*left*) and Teide (*right*) central vents (see text for details)

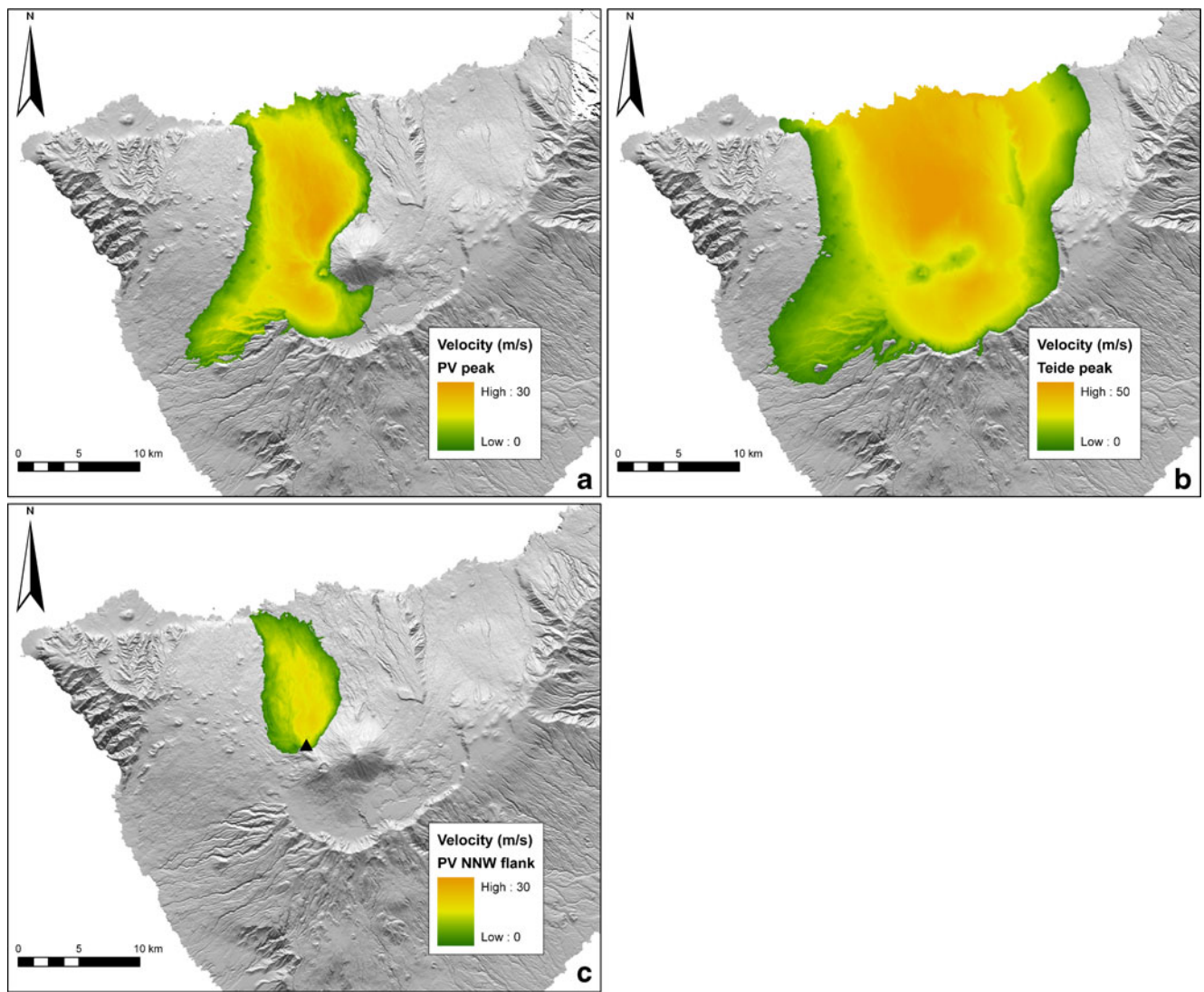


**Fig. 7** PDC scenarios. **a** Pico Viejo central vent, **b** Teide central vent and **c** vent located on black triangle (see text for details)

in this paper are violent strombolian, subplinian and plinian, which are the most significant ones in terms of probability of occurrence according to the long-term event trees published for TPV (Martí et al. 2008a; Sobradelo and Martí 2010). All the simulations were done considering a vent located in the northern flank of TPV at the same

distance from the two craters. The wind data used were obtained from a deep atmospheric sounding of an arbitrarily selected day (1 April 2010).

Plinian and subplinian events were simulated with the advection–diffusion model described in Folch and Felpeto (2005) considering the source term described by

**Table 4** Summary of the input parameters used in the simulations of ash fallout scenarios

Model	Violent strombolian FALL3D	Subplinian Folch and Felpeto (2005)	Plinian Folch and Felpeto (2005)
Column height	1.4 km	8 km	25 km
Volume emitted		0.05 km <sup>3</sup>	0.8 km <sup>3</sup>
Mass flow rate	5 × 10 <sup>4</sup> kg/s		
Duration	3 h		
Mean $\varphi/\varphi$ standard deviation	1/1	-2/1.5	0/1.5

the Suzuki (1983) expression. Simulation of violent strombolian eruption was computed with FALL3D 6.1 model (Costa et al. 2006). The input parameters for the subplinian eruption reproduce the best known explosive event of TPV, the Montaña Blanca eruption (Ablay et al. 1995; Folch and Felpeto 2005). Due to the lack of detailed data of deposits from the other two eruption types, the input parameters were chosen based on bibliographic data from other volcanoes. A summary of the input parameters is shown in Table 4. Figure 8 shows the results of the simulations.

### Validation of results

Based on existing geological data, we assessed the volcanic hazard for Teide–Pico Viejo as probabilities of occurrence

of at least one eruption exceeding a certain magnitude over different time periods. Like this, for example, given the data and assuming a future behaviour of the volcano similar to the past 10,000 years, we can say that in the next 50 years, there will be at least one eruption on TPV of magnitude  $M > 2$  with a probability of 11.1%. This probability jumps to 21.0% for the next 100 years, and a probability of 90.6% is obtained for the next 1,000 years (Table 3). The escalation rate is more significant in the first 500 years (Fig. 9).

To validate the model, we compared the probability results in Table 3 with the probability obtained from the Bayesian event tree model of Sobradelo and Martí (2010). The event tree was built to outline all possible eruptive scenarios at TPV and to assign a long-term probability of occurrence to each scenario. The Bayesian probabilities were computed only for the time window of 100 years. Therefore, when comparing with the results from the

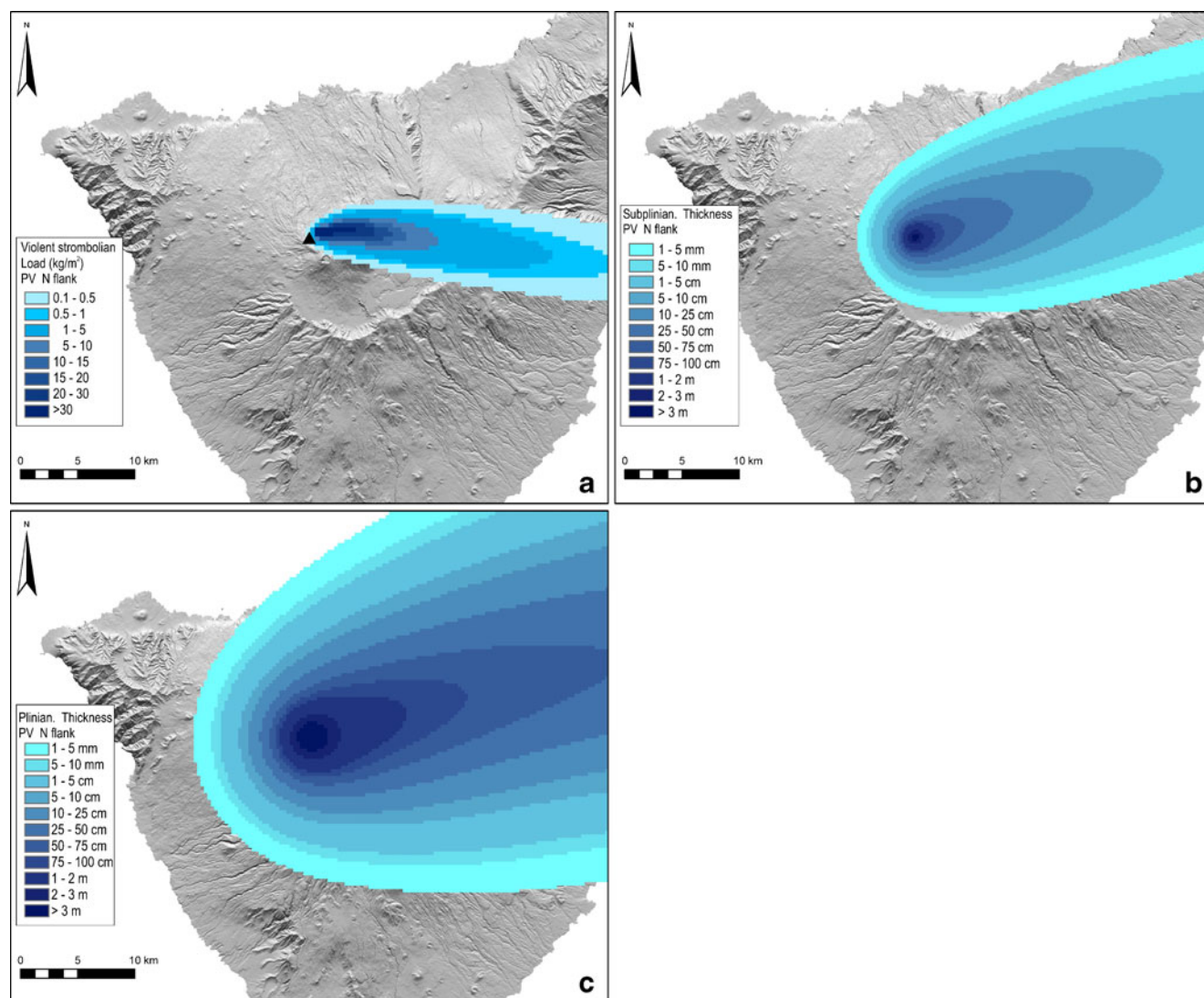


**Fig. 8** Ash fall scenarios. **a** Violent strombolian, **b** subplinian and **c** plinian (see text for details)

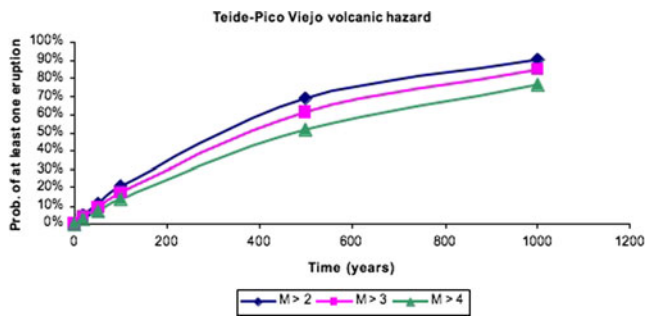


**Fig. 9** Probabilities calculated with NHGPPP of at least one eruption, with a size  $M$  greater than a given size threshold for the TPV eruptive series

extreme value theory method in Table 3, we can only compare the probabilities of an eruption of different sizes within one time window of 100 years. Table 5 shows on the second row the probabilities of having a magmatic unrest episode with magmatic eruption of phonolitic composition anywhere in the TPV during the next 100 years, computed using the Bayesian event tree model. The extreme value method was built using the number of eruptions occurring over time intervals, expressed in terms of the eruption occurrence rate for each class magnitude  $M$ , and extrapolated using the more complete records in the catalogue (Mendoza-Rosas and De la Cruz-Reyna 2008). The extreme value method takes into account the possible incompleteness of the data by extrapolating from the most reliable data points. The Bayesian model, on the other hand, is a subjective approach which starts with the state of total uncertainty and computes the final probabilities based on an incomplete data catalogue, without further adjustment. This explains why the Bayesian probability in Table 5 second row for magnitude  $>4$  (3.0%) falls abruptly relative to that for magnitude  $>3$  (11.2%). The NHGPPP gives more weight to the more extreme events, such as events of magnitude  $>4$  (13.6% versus 3.0%). For events of magnitude  $>2$ , the Bayesian probability (14.2%) is lower than the NHGPPP probability (21.1%) since the latter uses a larger number of extrapolated occurrences for events of magnitude 3, while the Bayesian method computes the results based on the single event registered in the catalogue. This comparison allows us to validate the consistency of the

**Table 5** Comparison of probability results from Bayesian event tree (Sobradelo and Martí 2010) and NHGPPP presented in this paper

Time (years)	$M > 2$ (%)	$M > 3$ (%)	$M > 4$ (%)	
100	21.1	17.3	13.6	Extreme value theory
100	14.2	11.2	3.0	Bayesian event tree

See text for explanation

probability results obtained here, but also reassures us in the choice of using the extreme value method to overcome the limitations in the data.

### Discussion

The TPV constitutes one of the main potentially active volcanic complexes in Europe but traditionally has not been considered to be explosive and to represent a significant threat to the island of Tenerife. However, the results obtained in this work suggest that hazard associated with TPV is not negligible and should be carefully considered in order to quantify volcanic risk in Tenerife.

Although NVEWS (Ewert et al. 2005) was specially designed to identify the level of monitoring required by US volcanoes in order to define an effective early warning system, it offers a simple approach for classifying active volcanoes according to their level of threat. In this sense, we consider NVEWS perfectly applicable to TPV, and the resulting value representative of the real level of threat TPV represents for Tenerife. The NVEWS analysis of volcanic threat, even assuming very conservative values for some of the evaluated factors, gives a value of 165, which classifies TPV as a very high threat volcano, comparable to Redoubt, Crater Lake or Augustine in the USA. It is worth mentioning that the level of volcano monitoring in Tenerife has improved significantly since 2004, when the Spanish Geographic Institute (IGN) implemented its multi-parametric surveillance network (see [www.ign.es](http://www.ign.es)), so that it can be said that TPV now has the required monitoring level that is appropriate to a very high threat volcano according to the NVEWS (Ewert et al. 2005).

Eruptions of volcanoes considered “dormant” or “inactive” have produced major disasters in the past. The volcanic hazard from volcanoes with a long recurrence interval tends to be ignored, especially when little or no historical data exist. This is the case for TPV. The probability results obtained here using extreme value theory, consistent with the results obtained in previous work using Bayesian inference, confirm once again the existence of significant volcanic hazard from TPV. This together with others signs of activity mentioned earlier should constitute sufficiently convincing reasons to accept that TPV is an active volcanic complex that may erupt again in the near future. Unfortunately, we have increasing evidence of the sudden awakening of long dormant volcanoes (e.g. Chichón 1982, Unzen 1991, Pinatubo 1991, Montserrat 1995–, Chaitén 2008). Conducting hazard assessment of volcanoes where knowledge of the past volcanological history is poor, geochronological data are scarce and there is not historical eruptive activity and is not an easy task. In these cases, the lack of knowledge of

previous unrest episodes and of the precursors to previous eruptive events precludes using repetitive patterns of precursors to anticipate new eruptions (see Sandri et al. 2004). This is the case at TPV, meaning that we do not know how a future reawakening would manifest and which could be the precursory patterns for new eruptions. Comparison with better known volcanoes, in particular with those that have erupted in recent times and from which we have good monitoring records, could help in predicting the future behaviour of TPV. However, experience demonstrates that each volcano has its own behaviour and that the definition and application of common patterns to interpret eruption precursors, particularly if we are dealing with composite volcanoes, should be done with care.

In the case of TPV, Martí et al. (2008a) indicated that its eruptive behaviour is controlled by the close relationship between deep basaltic and shallow phonolitic magma systems, to the extent that most of the TPV phonolitic products show evidence of magma mingling and/or mixing. From the existing radiometric ages and the stratigraphic relationships between the erupted products, it is clear that most of phonolitic eruptions are preceded by several basaltic eruptions and in some cases both occur simultaneously (e.g. Montaña Reventada, Araña et al. 1994; Wiesmaier et al. 2011). A similar pattern has also been observed in the pre-TPV central complex (Las Cañadas Edifice) (Martí et al. 2008a). Therefore, it is logical to infer that similar mechanisms have controlled the accumulation, evolution and eruption of magma at shallow levels during the past history of the Tenerife central complex, despite a progressive decrease in the magma available with time. In other words, the eruption of phonolitic magma at TPV is directly dependent on the amount of basaltic magma delivered at shallow depths into the central system. We then suggest that the eruption frequency at TPV is related to the eruption frequency of basaltic volcanism on Tenerife, which in historical times has produced eruptions in 1492, 1705, 1706, 1798 and 1909, with the last eruption from Teide dated at 1,150 years B.P. (Carracedo et al. 2007).

The main phonolitic erupted products of TPV correspond to lava flows that were emplaced towards the south into Las Cañadas depression and to the north in the Icod and La Orotava valleys. Most of the phonolitic lavas from TPV are clastogenic lavas formed by agglutination of large pyroclastic fragments generated in fire fountaining episodes. The rheological properties and flow behaviour of these lavas (Dingwell et al. 1998; Giordano et al. 2000; Gottsmann and Dingwell 2001) are characterised by a low viscosity at relatively low temperatures, which allow them to flow for long distances preserving an average thickness of tens of metres. In some cases, these lavas have flowed down into the Icod valley for more than 16 km reaching the coast, an area that today is highly populated. These lavas

typically preserve a considerable amount of magmatic gas. This is consistent with the relative large amount of volatiles found in the TPV phonolites (Ablay et al. 1995). An effect of this high content of gas in the TPV lavas is that they may transform into block and ash flows when they collapse gravitationally in slope breaks. Deposits of such pyroclastic density currents have been found in stratigraphic continuity with some lavas inside the gullies of the Icod valley, sometimes reaching the coast or being transformed into debris flow deposits at distal facies (García et al. 2011).

In addition to the fragmental origin of most of the TPV lavas and their occasional explosive transformation into pyroclastic density currents, there is evidence of larger explosive eruptions at TPV (García et al. 2011). This evidence is provided by the presence of discontinuous outcrops of pumice fall deposits, but their precise stratigraphic location in the TPV eruptive record is still not known. However, we can confirm that at least three phonolitic explosive eruptions of subplinian dimension, or perhaps even plinian, different from that of the already known Montaña Blanca eruption (Ablay et al. 1995; Folch and Felpeto 2005), have occurred from TPV during the Holocene. Moreover, the presence of ignimbrites is also confirmed in the eruption record of TPV, some of them with minimum run-out distances of several kilometres as it is indicated by the remnants of these deposits found in the Icod Valley, but which could have reached the coasts and entered the sea if we compare them with other ignimbrites of similar characteristics and volume (e.g. Calder et al. 1999; Loughlin et al. 2002). The ignimbrites may have derived either from collapse of eruption columns or from gravitational collapse of domes and clastogenic lava flows. This second option is certainly at least the origin for the block and ash deposits found in the Icod Valley, where the steep topography has facilitated such processes (García et al. 2011).

Therefore, we have considered in our analysis fall deposition and PDC hazards, in addition to lava flows, as representative of the potential hazards that might occur in a future eruption of TPV. The scenarios we have generated allow us to assess their potential extent. All these primary hazards would today easily reach the main populated areas to the north of TPV but could even reach other important locations on the other flanks in the case of plinian and subplinian fallout depending on wind direction.

In addition to the direct hazards that we have assumed in this paper, it is also important to take into account those hazards that could indirectly derive from a renewal of the eruptive activity at TPV. These mainly include debris flows and sector collapses, for which there is also evidence in the recent geological record. Some of the ignimbrites from TPV show evidence of syn-depositional erosion which suggest that heavy rainfalls may have occurred in the area

during these eruptions (García et al. 2011). It is also significant that at the north of Tenerife, important seasonal rainfalls contribute to the erosion and remobilisation of the unconsolidated volcanic material, forming important debris flows. The existence of small-scale sector collapses at the north flank of TPV has also been pointed out by previous authors (Ablay and Martí 2000; Ablay and Hürlimann 2000)

In this study, we have only considered the phonolitic eruptions, as they have the potential to generate the most important hazards at TPV, but it is worth noting that basaltic eruptions have also occurred at this volcanic complex. Most of these eruptions have been strombolian to violent strombolian and have generated lava flows with a variable extent and restricted scoria lapilli deposits. Some significant phreatomagmatic episodes have also occurred related at the former craters of Teide and the present one in the case of Pico Viejo (Ablay and Martí 2000; Perez-Torrado et al. 2004). These phreatomagmatic eruptions produced high-energy pyroclastic surges that flowed to the north for several kilometres into the Icod valley. The extent of these deposits is similar to some of the phonolitic PDCs from TPV, so the hazard scenarios we have developed for phonolitic PDCs also apply to potential basaltic surges emplaced towards the north of TPV.

## Conclusions

In this study, we have presented the temporal and spatial probabilities for a phonolitic eruption at TPV and have discussed their implications in terms of hazard assessment. The computation of both temporal and spatial probabilities of a phonolitic eruption at TPV and the characterization of the main expected scenarios constitute the fundamental basis for building up the phonolitic hazard maps for TPV. An important conclusion we can draw from these results is that TPV has to be identified as a volcanic complex that may pose serious hazard on the island of Tenerife and in particular to its northern side. The hazard scenarios we have simulated show that the southern flank of Tenerife is protected by the Cañadas caldera wall against lava flows and pyroclastic density currents, but not against ash fallout. The Icod Valley, and in a minor extent also the La Orotava valley, is directly exposed to most of TPV hazards, in particular to the gravity driven flows, due to the steep topography of that side of the island and the lack of topographic barriers. According to these results and to the fact that Tenerife is a densely populated island, it is strongly recommended that preparedness plans, emergency and disaster management procedures be put into place to quickly react and minimise loss during a volcanic crisis.

**Acknowledgements** This research has been in part funded by MICINN grant CGL2008-04264 and by a IGN-CSIC collaboration agreement. We thank the National Park of Teide for giving us permission to undertake this research. Many thanks to Laura Sandri and Olivier Jacquet for their constructive reviews

## References

- Ablay GJ, Hürlimann M (2000) Evolution of the north flank of Tenerife by recurrent giant landslides. *J Volcanol Geotherm Res* 103:135–159
- Ablay GJ, Martí J (2000) Stratigraphy, structure, and volcanic evolution of the Pico Teide–Pico Viejo formation, Tenerife, Canary Islands. *J Volcanol Geotherm Res* 103:175–208
- Ablay GJ, Ernst GGJ, Martí J, Sparks RJ (1995) The 2 ka subplinian eruption of Montaña Blanca, Tenerife. *Bull Volcanol* 57:337–355
- Ablay GJ, Carroll MR, Palmer MR, Martí J, Sparks RSJ (1998) Basanite–phonolite lineages of the Teide–Pico Viejo volcanic complex, Tenerife, Canary Islands. *J Petrol* 39:905–936
- Araña V, Martí J, Aparicio A, García-Cacho L, García-García R (1994) Magma mixing in alkaline magmas: an example from Tenerife (Canary Islands). *Lithos* 32:1–19
- Calder ES, Cole PD, Dade WB, Druitt TH, Hoblitt RP, Huppert HE, Ritchie L, Sparks RSJ, Young SR (1999) Mobility of pyroclastic flows and surges at the Soufriere Hills Volcano, Montserrat. *Geophys Res Lett* 26:537–540
- Carracedo JC (1994) The Canary Islands: an example of structural control on the growth of large oceanic-island volcanoes. *J Volcanol Geotherm Res* 60:225–241
- Carracedo JC, Paterne M, Guillou H, Pérez-Torrado FJ, Paris R, Rodríguez-Badiola E, Hansen A (2003) Dataciones radiométricas (14C y K/Ar) del Teide y el rift noroeste, Tenerife, Islas Canarias. *Est Geol* 59:15–29
- Carracedo JC, Rodríguez-Badiola E, Guillou H, Paterne M, Scaillet S, Pérez-Torrado FJ, Paris R, FraPaleo U, Hansen A (2007) Eruptive and structural history of Teide volcano and rift zones of Tenerife, Canary Islands. *Geol Soc Am Bull* 119:1027–1051
- Carracedo JC, Guillou H, Nomade S, Rodríguez-Badiola E, Pérez-Torrado FJ, Rodríguez-González A, Paris R, Troll VR, Wiesmaier S, Delcamp A, Fernández-Turiel JL (2010) Evolution of ocean-island rifts: The northeast rift zone of Tenerife, Canary Islands. *Geol Soc Am Bull*. doi:10.1130/B30119.1
- Coles S (ed) (2001) An introduction to statistical modeling of extreme values. Springer, London, p 228
- Connor CB, Hill BE (1995) Three nonhomogeneous Poisson models for the probability of basaltic volcanism: application to the Yucca Mountain region. *J Geophys Res* 100:10,107–10,125
- Costa A, Macedonio G, Folch A (2006) A three-dimensional Eulerian model for transport and deposition of volcanic ashes. *Earth Planet Sci Lett* 241:634–664
- Davison A, Smith R (1990) Models for exceedances over high thresholds. *J Roy Stat Soc* 52:393–442
- Del Potro R, Hürlimann M (2008) Geotechnical classification and characterisation of materials for stability analyses of large volcanic slope. *Engi Geol* 98:1–17
- Dingwell DB, Hess KU, Romano C (1998) Extremely fluid behavior of hydrous peralkaline rhyolites. *Earth Planet Sci Lett* 158:31–38
- Domínguez Cerdeña I, Del Fresno C, Rivera L (2011) New insight on the increasing seismicity during Tenerife's 2004 volcanic reactivation. *J Volcanol Geotherm Res* 206:15–29
- Ewert J, Guffanti M, Murray T (2005) An assessment of volcanic threat and monitoring capabilities in the United States—framework for a National Volcanic Early Warning System, NVEWS. *US Geol Surv Open-File Rep* 1164:1–62

- Felpeto A, Araña V, Ortiz R, Astiz M, García A (2001) Assessment and modelling of lava flow hazard on Lanzarote (Canary Islands). *Nat Haz* 23:247–257. doi:10.1023/A:1011112330766
- Felpeto A, Martí J, Ortiz R (2007) Automatic GIS-based system for volcanic hazard assessment. *J Volcanol Geotherm Res* 166:106–116
- Folch A, Felpeto A (2005) A coupled model for dispersal of tephra during sustained explosive eruptions. *J Volcanol Geotherm Res* 145:337–349
- García A, Vila J, Ortiz R, Macià R, Sleeman R, Marrero JM, Sánchez N, Tárrega M, Correig AM (2006) Monitoring the reawakening of Canary Island's Teide volcano. *EOS Trans* 87(61):65
- García O, Martí J, Aguirre-Díaz G, Geyer A, Iribarren I (2011) Pyroclastic density currents from Teide–Pico Viejo (Tenerife, Canary Islands): implications on hazard assessment. *TerraNova* 23:220–224. doi:10.1111/j.1365-3121.2011.01002.x
- Giordano D, Dingwell DB, Romano C (2000) Viscosity of a Teide phonolite in the welding interval. *J Volcanol Geotherm Res* 103:239–245
- Gottsmann J, Dingwell DB (2001) Cooling dynamics of spatter-fed phonolite obsidian flows on Tenerife, Canary Islands. *J Volcanol Geotherm Res* 105:323–342
- Gottsmann J, Wooller L, Martí, Fernandez J, Camacho A, González P, García A, Rymer H (2006) New evidence for the reawakening of Teide volcano. *Geophys Res Lett* 33(L20311). doi:10.1029/2006GL027523
- Hernández PA, Pérez N, Salazar JML, Nakai S, Notsu K, Wakita H (1998) Diffuse emission of carbon dioxide, methane and helium-3 from Teide volcano, Tenerife, Canary Islands. *Geophys Res Lett* 25:3311–3314
- Kinvisg HS, Winson A, Gottsmann J (2010) Analysis of volcanic threat from Nisyros Island, Greece, with implications for aviation and population exposure. *Nat Haz Earth Syst Sci* 10:1101–1113
- Loughlin SC, Calder ES, Clarke A, Cole PD, Luckett R, Mangan MT, Pyle DM, Sparks RSJ, Voight B, Watts RB (2002) Pyroclastic flows and surges generated by the 25 June 1997 dome collapse, Soufriere Hills Volcano, Montserrat. In: Druitt TH, Kokelaar BP (eds) *The eruption of Soufriere Hills Volcano, Montserrat, from 1995 to 1999*. *Mem Geol Soc London* 21. Geological Society of London, London, pp 191–209
- Malin MC, Sheridan MF (1982) Computer-assisted mapping of pyroclastic surges. *Science* 217:637–639
- Martí J, Felpeto A (2010) Methodology for the computation of volcanic susceptibility. An example for mafic and felsic eruptions on Tenerife (Canary Islands). *J Volcanol Geotherm Res* 195:69–77
- Martí J, Geyer A (2009) Central vs flank eruptions at Teide–Pico Viejo twin stratovolcanoes (Tenerife, Canary Islands). *J Volcanol Geotherm Res* 181:47–60
- Martí J, Gudmundsson A (2000) The Las Cañadas caldera (Tenerife, Canary Islands): an overlapping collapse caldera generated by magma-chamber migration. *J Volcanol Geotherm Res* 103:161–173
- Martí J, Mitjavila J, Araña V (1994) Stratigraphy, structure and geochronology of the Las Cañadas caldera (Tenerife, Canary Islands). *Geol Mag* 131:715–727
- Martí J, Hurlimann M, Ablay GJ, Gudmundsson A (1997) Vertical and lateral collapses in Tenerife and other ocean volcanic islands. *Geology* 25:879–882
- Martí J, Aspinall WP, Sobradelo R, Felpeto A, Geyer A, Ortiz R, Baxter P, Cole P, Pacheco JM, Blanco MJ, Lopez C (2008a) A long-term volcanic hazard event tree for Teide-Pico Viejo stratovolcanoes (Tenerife, Canary Islands). *J Volcanol Geotherm Res* 178:543–552
- Martí J, Geyer A, Andujar Teixó F, Costa F (2008b) Assessing the potential for future explosive activity from Teide–Pico Viejo stratovolcanoes (Tenerife, Canary Islands). *J Volcanol Geotherm Res* 178:529–542
- Martí J, Ortiz R, Gottsmann J, García A, De La Cruz-Reyna S (2009) Characterising unrest during the reawakening of the central volcanic complex on Tenerife, Canary Islands, 2004–2005, and implications for assessing hazards and risk mitigation. *J Volcanol Geotherm Res* 182:23–33
- Martin AJ, Umeda K, Connor CB, Weller JN, Zhao D, Takahashi M (2004) Modeling long-term volcanic hazards through Bayesian inference: an example from the Tohoku volcanic arc, Japan. *J Geophys Res* 109:B10208
- Marzocchi W, Sandri L, Selva J (2010) BET\_VH: a probabilistic tool for long-term volcanic hazard assessment. *Bull Volcanol* 72:705–716. doi:10.1007/s00445-010-0357-8
- Mendoza-Rosas AT, De la Cruz-Reyna S (2008) A statistical method linking geological and historical eruption time series for volcanic hazard estimations: applications to active polygenetic volcanoes. *J Volcanol Geotherm Res* 176:277–290
- Newhall CG, Self S (1982) The volcanic explosivity index (VEI): an estimate of the explosive magnitude for historical eruptions. *J Geophys Res* 87:1231–1238
- Pérez NM, Coello C, Marrero R, González Y, Brrancos PJ (2005) Premonitory geochemical and geophysical signatures of volcanic unrest at Tenerife, Canary Islands. *Geophys Res Abst* 7:09993, SRef-ID: 1607-7962/gra/EGU05-A-09993
- Perez-Torrado FJ, Carracedo JC, Paris R, Hansen A (2004) Descubrimiento de depósitos freatomagmáticos en la laderas septentrionales del estratovolcán Teide (Tenerife, Islas Canarias): relaciones estratigráficas e implicaciones volcánicas. *Geotemas* 6:163–166
- Pyle DM (2000) Sizes of volcanic eruptions. In: Sigurdsson H (ed) *Encyclopedia of volcanoes*. Academic, San Diego, pp 263–269
- Rodríguez-Losada J, Hernández-Gutiérrez LE, Olalla C, Perucho A, Serrano A, Eff-Darwich A (2009) Geomechanical parameters of intact rocks and rock masses from the Canary Islands: implications on their flank stability. *J Volcanol Geotherm Res* 182:67–75
- Sandri L, Marzocchi W, Zaccarelli L (2004) A new perspective in identifying the precursory patterns of eruptions. *Bull Volcanol* 66:263–275
- Sheridan MF, Malin MC (1983) Application of computer-assisted mapping to volcanic hazard evaluation of surge eruption: Vulcano, Lipari, Vesuvius. *Explosive volcanism*. *J Volcanol Geotherm Res* 17:187–202
- Sobradelo R, Martí J (2010) Bayesian event tree for long-term volcanic hazard assessment: application to Teide-Pico Viejo stratovolcanoes, Tenerife, Canary Islands. *J Geophys Res* 115: B05206. doi:10.1029/2009JB006566
- Sobradelo R, Martí J, Mendoza-Rosas AT, Gómez G (2011) Volcanic hazard assessment for the Canary Islands (Spain) using extreme-event statistics. *Nat Hazards Earth Syst Sci* 11:2741–2753. doi:10.5194/nhess-11-2741-2011
- Suzuki T (1983) A theoretical model for dispersion of tephra. In: Shimozuru D, Yokoyama I (eds) *Arc volcanism: physics and tectonics*. Terra Scientific, Tokyo, pp 95–113
- Toyos G, Cole P, Felpeto A, Martí J (2007) A GIS-based methodology for hazard mapping of small volume pyroclastic density currents. *Nat Haz* 41:99–112
- Wiesmaier S, Deegan FM, Troll VR, Carracedo JC, Chadwick JP, Chew DM (2011) Magma mixing in the 1100 AD Montaña Reventada composite lava flow, Tenerife, Canary Islands: interaction between rift zone and central volcano plumbing system. *Contrib Mineral Petrol*. doi:10.1007/s00410-010-0596-x